

3 1176 00085 1759

~~RESTRICTED~~

UNCLASSIFIED

Copy 5
RM L50E12a

NACA RM L50E12a



Ref 19

1154
754
2.1

RESEARCH MEMORANDUM

EFFECT OF VARIOUS OUTBOARD AND CENTRAL FINS ON LOW-SPEED
YAWING STABILITY DERIVATIVES OF A 60° DELTA-WING MODEL

By Alex Goodman

Langley Aeronautical Laboratory
Langley Air Force Base, Va.

CLASSIFICATION CANCELLED

Authorized by J. W. Crowley Date 12/11/55

J. E. O. J. O. 5017

By DATA 1/13/54 488 MAEL

CLASSIFIED DOCUMENT

R7 1864

This document contains classified information affecting the National Defense of the United States within the meaning of the Espionage Act, USC 8031 and 32. Its transmission or the revelation of its contents in any manner to an unauthorized person is prohibited by law. Information so classified may be imparted only to persons in the military and naval services of the United States, appropriate civilian officers and employees of the Federal Government who have a legitimate interest therein, and to United States citizens of known loyalty and discretion who of necessity must be informed thereof.

AERONAUTICAL LIBRARY
LANGLEY AERONAUTICAL LABORATORY
Langley Field, Va.

NATIONAL ADVISORY COMMITTEE FOR AERONAUTICS

WASHINGTON

June 19, 1950

UNCLASSIFIED

~~RESTRICTED~~

NATIONAL ADVISORY COMMITTEE FOR AERONAUTICS

RESEARCH MEMORANDUM

EFFECT OF VARIOUS OUTBOARD AND CENTRAL FINS ON LOW-SPEED
YAWING STABILITY DERIVATIVES OF A 60° DELTA-WING MODEL

By Alex Goodman

SUMMARY

An investigation has been conducted in the 6- by 6-foot curved-flow test section of the Langley stability tunnel in order to determine the effects of various outboard and central fins on the low-speed yawing stability derivatives of a triangular-wing model.

The results of the investigation indicated that the highest-aspect-ratio central fin in the rear position contributed more damping in yaw C_{nr} per unit area and maintained its effectiveness in producing damping in yaw to higher lift coefficients than the lower-aspect-ratio central fins and the outboard fins. The effect of lateral movement of the outboard fins on the yawing stability derivatives was fairly small. The effect of the outboard fins on the damping in yaw at low lift coefficients could be predicted by use of elementary concepts.

In order to predict the effects of central fins on the yawing stability derivatives by use of simple theoretical expressions it was found necessary to employ an effective center of pressure of the load contributed by the fin.

INTRODUCTION

A systematic program has been initiated by the National Advisory Committee for Aeronautics for experimentally determining the static and rotary derivatives of various wings and complete airplane configurations. The rolling-flow and curved-flow equipment of the Langley stability tunnel (references 1 and 2) is being used to determine the rotary derivatives. As part of this program, several triangular-wing models are being investigated. The static and rolling characteristics of one triangular-wing model is reported in reference 3.

The present investigation was conducted in order to determine the effects of several central and outboard fin configurations on the low-speed yawing stability characteristics of the triangular-wing model of reference 3.

Comparisons of the effectiveness of the various fins in producing damping in yaw are made, and curves showing the variation of the effective center-of-pressure location of the central fins with angle of attack are presented. A procedure is suggested for employing these centers of pressure in calculating the contribution of central fins to the various stability derivatives of similar model configurations.

SYMBOLS

The data presented herein are in the form of standard NACA coefficients of forces and moments which are referred to the stability system of axes with the origin at the calculated aerodynamic center of the wing. The positive direction of the forces, moments, and angular displacements are shown in figure 1. The coefficients and symbols used herein are defined as follows:

$$C_L \quad \text{lift coefficient} \quad \left(\frac{\text{Lift}}{\frac{1}{2}\rho V^2 S} \right)$$

$$C_Y \quad \text{lateral-force coefficient} \quad \left(\frac{\text{Lateral force}}{\frac{1}{2}\rho V^2 S} \right)$$

$$C_l \quad \text{rolling-moment coefficient} \quad \left(\frac{\text{Rolling moment}}{\frac{1}{2}\rho V^2 S b} \right)$$

$$C_n \quad \text{yawing-moment coefficient} \quad \left(\frac{\text{Yawing moment}}{\frac{1}{2}\rho V^2 S b} \right)$$

$$C_{L\alpha} = \frac{\partial C_L}{\partial \alpha}$$

$$C_{Yr} = \frac{\partial C_Y}{\partial \left(\frac{rb}{2V} \right)}$$

$$C_{L_r} = \frac{\partial C_L}{\partial \left(\frac{rb}{2V}\right)}$$

$$C_{n_r} = \frac{\partial C_n}{\partial \left(\frac{rb}{2V}\right)}$$

$$C_{Y_\beta} = \frac{\partial C_Y}{\partial \beta}$$

$$C_{L_\beta} = \frac{\partial C_L}{\partial \beta}$$

$$C_{n_\beta} = \frac{\partial C_n}{\partial \beta}$$

$$C_{L_\psi} = \frac{\partial C_L}{\partial \psi}$$

$$C_{Y_\psi} = \frac{\partial C_Y}{\partial \psi}$$

$$C_{n_\psi} = \frac{\partial C_n}{\partial \psi}$$

ρ mass density of air, slugs per cubic foot

V free-stream velocity, feet per second

S area, feet

b span, feet

A aspect ratio (b^2/S)

c chord parallel to plane of symmetry, feet

\bar{c} mean aerodynamic chord, feet $\left(\frac{2}{S} \int_0^{b/2} c^2 dy\right)$

\bar{z} perpendicular distance from fuselage center line to center of pressure of fin, feet

l	longitudinal distance from center of gravity to fin center of pressure, feet
x	longitudinal distance along fuselage center line, feet
α	angle of attack, degrees
β	angle of sideslip, radians ($-\psi$)
ψ	angle of yaw, degrees
Λ	angle of sweepback of quarter-chord line, degrees
$\Lambda_{L.E.}$	angle of sweepback of leading edge, degrees
R	Reynolds number
λ	taper ratio $\left(\frac{\text{Tip chord}}{\text{Root chord}} \right)$
$\frac{rb}{2V}$	yawing-velocity parameter
r	yawing angular velocity, radians per second
Subscripts:	
w	wing
t	fin

APPARATUS, MODEL, AND TESTS

The tests of the present investigation were conducted in the 6- by 6-foot curved-flow test section of the Langley stability tunnel. In this test section curved flight is simulated by directing the air in a curved path about a fixed model (reference 2).

All the component parts of the model were constructed of laminated mahogany, and all surfaces were given a polished lacquer finish. The wing had an angle of sweepback of the leading edge of 60° , a modified NACA 65(06)-006.5 airfoil section parallel to the plane of symmetry, and an aspect ratio of 2.31 (fig. 2). Photographs of several of the model configurations tested are presented as figure 3.

Outboard fins of $A_t = 1.5$ and $A_t = 1.4$ were tested in the spanwise positions shown in figures 4(a) and 4(b), respectively. Single central vertical fins having aspect ratios of 0.77, 1.15, and 2.31 were tested on the fuselage in the two positions shown in figure 5. A summary of these test configurations is given in table I. The rolling-moment, yawing-moment, and lateral-force coefficients were determined for each configuration by testing each model configuration through an angle-of-attack range from $\alpha = -4^\circ$ to beyond maximum lift at values of $rb/2V$ of 0, -0.032, -0.067, and -0.088. The variation of the rolling-moment, yawing-moment, and lateral-force coefficients with $rb/2V$ are the stability derivatives C_{l_r} , C_{n_r} , and C_{Y_r} , respectively.

The outboard fin of $A_t = 1.4$ (position 3) and central fin of $A_t = 2.31$ in the rearward position were tested through an angle-of-yaw range for the aforementioned negative values of $rb/2V$ at several angles of attack in order to determine the variation of C_{Y_r} , C_{n_r} , and C_{l_r} with ψ . Results for positive values of $rb/2V$ and positive values of ψ were obtained by assuming that the model was symmetrical about the XZ-plane and by utilizing the results for the corresponding opposite angles of yaw and $rb/2V$ with regard for signs. This procedure amounted to averaging the derivatives for corresponding positive and negative angles of yaw. The values presented in this paper are these average values.

The test Reynolds number and Mach number were 1.624×10^6 and 0.13, respectively.

CORRECTIONS

Corrections for the effects of jet boundaries, based on unswept-wing theory, have been applied to the angle-of-attack and rolling-moment-coefficient data.

The lateral-force coefficient has been corrected for the buoyancy effect of the static-pressure gradient associated with curved flow.

No correction for the effects of blocking or support-strut interference has been applied.

RESULTS AND DISCUSSION

Presentation of Results

The results of the present series of tests are given in figures 6 to 13. The variation of lift coefficient with angle of attack for the

wing, wing-fuselage combination, and for each wing-fuselage-fin combination is presented in figure 6. The static and rolling characteristics for this model are presented in reference 3. The yawing stability derivatives obtained for the wing, wing-fuselage combination, and for each wing-fuselage-fin combination are presented in figures 7 to 11. The variation of the yawing stability derivatives with angle of yaw for two fin configurations is given in figure 12. Table I summarizes the various model configurations and figures where the data are presented.

The variation of the calculated effective center of pressure with angle of attack for several of the central vertical fins is presented in figure 13.

Wing and Wing-Fuselage Results

The lift-curve variations obtained for the wing and wing-fuselage combination presented in figure 6 are very similar to the results presented in reference 3.

The effect of the fuselage on C_{nr} and C_{lr} was very small over most of the lift-coefficient range (fig. 7). Beyond a lift coefficient of about 0.65, C_{lr} for the wing-fuselage combination becomes more negative than for the wing alone. This change occurs for the same lift-coefficient range as the reduction in lift-curve slope and the decrease in $C_{l\psi}$ caused by the addition of the fuselage to the wing as shown in figure 6 and in reference 3, respectively.

Effect of Outboard Fins

Symmetrical outboard fins.— The addition of the fins of $A_t = 1.5$ to the model in either position 1 or 2 (fig. 4(a)) caused negative increments of C_{nr} and positive increments of C_{Yr} as would be expected. The effect on C_{nr} of shifting the fins inboard is very small at low lift coefficients but causes approximately a 50-percent decrease in C_{nr} at a lift coefficient of 0.5. The contribution of the outboard fins to C_{nr} and C_{Yr} can be determined at low lift coefficients with good accuracy from equations based on elementary considerations. (See table II.) The equations employed for estimating the effects of the vertical fins (reference 4) are

$$\Delta C_{Yrt} = 2 \frac{l}{b} C_{Y\beta t} \quad (1)$$

$$\Delta C_{nr_t} = -2 \left(\frac{l}{b} \right)^2 C_{Y\beta t} \quad (2)$$

where the center of pressure is assumed to be at the quarter-chord point of the mean aerodynamic chord of the outboard fin.

The effects on C_{L_r} of shifting the fins inboard are small and poorly defined for lift coefficients below $C_L = 0.6$. At $C_L = 0.63$, a sharp break in C_{L_r} occurred for the inboard fin position (position 2). This break corresponds to the decrease in lift-curve slope obtained at the same lift coefficient (fig. 6). Breaks also appear in the curves of C_{N_r} and C_{Y_r} at $C_L = 0.63$. The phenomenon which causes these irregularities is discussed in the following section.

Upper-surface outboard fins.— Mounting the upper-surface outboard fins at $A_t = 1.4$ shown in figure 4(b) on the model caused appreciably larger increments in C_{N_r} and C_{Y_r} at low and moderate lift coefficients than were obtained with the smaller symmetrical fins, as would be expected (figs. 8 and 9). The effect on C_{N_r} and C_{Y_r} of shifting the fins inboard is very small below a lift coefficient of 0.6.

The contribution of the upper-surface outboard fins to C_{N_r} and C_{Y_r} (table II) can be determined with good accuracy at low lift coefficients by equations (1) and (2).

The addition of the upper-surface outboard fins caused an appreciable positive shift in C_{L_r} at $C_L = 0$. As in the case of the symmetrical outboard fins, a partial stall occurs at $C_L = 0.48$ when the upper-surface fins are moved inboard from position 1 to position 2 and at $C_L = 0.6$ when they are moved to position 3 (fig. 9). The partial stalling is also indicated by the decreases in $C_{L_{\alpha}}$ and the irregularities in C_{N_r} and C_{Y_r} at the same lift coefficients for fin positions 2 and 3 (figs. 6 and 9).

An explanation for these breaks has been advanced in reference 3. Results of tuft studies (reference 3) indicated that a sudden flow reversal (stalling) occurred just outboard of the fins in either position 2 or 3. Pressure-distribution investigations reported in reference 5 show that two semispan vortices, which exist for wings of triangular plan form, are swept inward from the tips as the angle of attack is increased. It appears that when these vortices approach the fins, the fins are subjected to such large induced angles that sudden stalling of the fins occurs and thus the portion of the wing outboard of the fins stalls. As the fins are moved inboard, the contact of the vortex and the fin is delayed until a higher angle of attack; but when stalling does occur, the adverse effect is greater since the area outboard of the fin is larger.

Effect of Central Fins

The addition of the central fins to the wing-fuselage combination (fig. 5) had very little effect on the lift characteristics of the model as can be seen in figure 6.

The effect of the various central fins on C_{n_r} , C_{l_r} , and C_{y_r} is similar in many respects to their effects on C_{n_ψ} , C_{l_ψ} , and C_{y_ψ} given in reference 3. In general, the effectiveness per unit area of the central fins increased as the size of the fins increased. All the central fins in the forward position produced negative increments of C_{n_r} and positive increments of C_{l_r} and C_{y_r} as would be expected. Moving the fins rearward generally accentuated these effects except for the smallest fin ($A = 0.77$) in the rearward position where the increment of C_{l_r} contributed by the fin was negative above $C_L = 0.1$.

A comparison of the values of C_{n_r} obtained for the outboard and central fins indicates that the loss in C_{n_r} at high lift coefficients is smaller for all forward and rearward central fins than for the outboard fins. Of all the fins investigated, the central fin ($A_t = 2.31$ in rearward position) was found to be the most effective for producing C_{n_r} on the basis of equal areas.

Effects of Yaw

The variation of the derivatives C_{n_r} and C_{y_r} with ψ for the central fin ($A_t = 2.31$ in rearward position) and the outboard fin ($A_t = 1.4$ in position 3) is fairly small through the yaw range for the angles of attack investigated (fig. 12). The central fin shows a fairly large percentage change in C_{l_r} with ψ , but little or no change occurs in the variation of C_{l_r} with ψ for the outboard fin (fig. 12).

Effective Center-of-Pressure Location for

Central Vertical Fins

Because of the proximity of the central vertical fins to the wing and consequently a lack of knowledge of the effective tail length, it was found difficult to make simple estimations of the tail contribution. The results of these tests have thus been converted to the form of effective centers of pressure of the vertical surfaces from which estimates of tail contributions to the yawing derivatives may be made by use of the considerations of reference 4. The equations for the tail contribution to C_{n_r} (equation (2)) and to C_{l_r}

$$\Delta C_{l_{rt}} = 2 \frac{l}{b} \left(\frac{\bar{z}}{b} - \frac{l}{b} \sin \alpha \right) C_{Y_{\beta t}} \quad (3)$$

were used as a basis for calculating the effective centers of pressure of the vertical surfaces.

Equations (2) and (3) were solved for the factors l/b and \bar{z}/b for several angles of attack, using experimental values of $\Delta C_{n_{rt}}$, $\Delta C_{l_{rt}}$, and $C_{Y_{\beta t}}$. The values obtained for l/b and \bar{z}/b for the central vertical fins are presented in figure 13.

By using equations (2) and (3), the results of figure 13, and either experimental or estimated values of $C_{Y_{\beta t}}$, the contributions of fins to the values of $C_{n_{rt}}$ and $C_{l_{rt}}$ may be estimated for model configurations similar to those employed for these tests. Values of l/b and \bar{z}/b can be obtained for triangular fins having aspect ratios from 0.77 to 2.31 by interpolating the results of figure 13. These values of l/b and \bar{z}/b are expected to apply only to fin-wing combinations having area ratios S_t/S_w close to those of the fin-wing combinations presented.

Experimental values of $C_{Y_{\beta t}}$ are preferable for calculations of the nature discussed herein. However, if experimental values are not available, theoretical values of the tail lift-curve slope $C_{L_{\alpha t}}$ can be obtained from references 6 and 7 and $C_{Y_{\beta t}}$ can be estimated by

$$C_{Y_{\beta t}} = 57.3 C_{L_{\alpha t}} \frac{S_t}{S_w} \quad (4)$$

As shown in figure 13, the effective centers of pressure move rearward with respect to the calculated aerodynamic center (\bar{c}_t/l) of the fin as the fin is moved forward. This effect is probably caused by the change in relative importance of the loading resulting from the curvature of the flight path. In most cases the effective center of pressure was approximately at the center of area of the fin.

CONCLUSIONS

An investigation of the low-speed yawing stability derivatives of a triangular-wing model with various fin arrangements indicated the following conclusions:

1. The highest-aspect-ratio central fin in the rear position contributed more damping in yaw C_{n_r} per unit area than any of the lower-aspect-ratio central or outboard fins tested. The central fins maintained their effectiveness in producing damping in yaw to higher lift coefficients than the outboard fins.

2. The effect of the lateral movement of the outboard fins on the yawing stability derivatives was fairly small at low lift coefficients but became more important at higher lift coefficients. The contribution of the outboard fins to the damping in yaw at low lift coefficients could be predicted by use of elementary concepts.

3. The variation of the yawing stability derivatives with angle of yaw for several fin configurations was generally found to be small for the angle-of-attack range investigated.

4. In order to predict the effects of central fins on the yawing stability derivatives by simple theoretical expressions it was found necessary to employ an effective center of pressure of the load contributed by the fin. The calculated effective center of pressure of the central fins was found to move rearward with respect to the quarter-chord point of the fin mean aerodynamic chord as the fin was moved forward on the fuselage.

Langley Aeronautical Laboratory
National Advisory Committee for Aeronautics
Langley Air Force Base, Va.

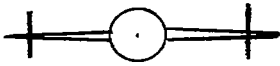
REFERENCES

1. MacLachlan, Robert, and Letko, William: Correlation of Two Experimental Methods of Determining the Rolling Characteristics of Unswept Wings. NACA TN 1309, 1947.
2. Bird, John D., Jaquet, Byron M., and Cowan, John W.: Effect of Fuselage and Tail Surfaces on Low-Speed Yawing Characteristics of a Swept-Wing Model as Determined in Curved-Flow Test Section of Langley Stability Tunnel. NACA RM L8G13, 1948.
3. Jaquet, Byron M., and Brewer, Jack D.: Effects of Various Outboard and Central Fins on Low-Speed Static-Stability and Rolling Characteristics of a Triangular-Wing Model. NACA RM L9E18, 1949.
4. Bamber, Millard J.: Effect of Some Present-Day Airplane Design Trends on Requirements for Lateral Stability. NACA TN 814, 1941.
5. Anderson, Adrien E.: Chordwise and Spanwise Loadings Measured at Low Speed on Large Triangular Wings. NACA RM A9B17, 1949.
6. Murray, Harry E.: Wind-Tunnel Investigation of End-Plate Effects of Horizontal Tails on a Vertical Tail Compared with Available Theory. NACA TN 1050, 1946.
7. DeYoung, John: Theoretical Additional Span Loading Characteristics of Wings with Arbitrary Sweep, Aspect Ratio, and Taper Ratio. NACA TN 1491, 1947.

TABLE I.- CONFIGURATIONS INVESTIGATED

Configuration	Fin aspect ratio, A_t	Area ratio, S_t/S_w	Fin location	Figure
	1.5	0.083	Outboard 0.83 b/2	} 8
	1.5	0.083	0.50 b/2	
	1.4	0.22	0.74 b/2	} 9
	1.4	0.22	0.63 b/2	
	1.4	0.22	0.50 b/2	
	0.77	0.33	} Central	} 10
	1.15	0.50		
	2.31	0.25		
	0.77	0.33	} Rear	} 11
	1.15	0.50		
	2.31	0.25		

TABLE II.— COMPARISON OF EXPERIMENTAL AND CALCULATED
VALUES OF $\Delta C_{n_{rt}}$ AND $\Delta C_{Y_{rt}}$ AT $C_L = 0$

Configuration	Experimental			Calculated	
	$C_{Y_{\beta t}}$	$\Delta C_{n_{rt}}$	$\Delta C_{Y_{rt}}$	$\Delta C_{n_{rt}}$	$\Delta C_{Y_{rt}}$
	0.177	-0.05	0.11	-0.046	0.127
	.115	-.05	.08	-.040	.111
	.550	-.220	.45	-.204	.47
	.562	-.240	.45	-.208	.48
	.573	-.210	.42	-.212	.49

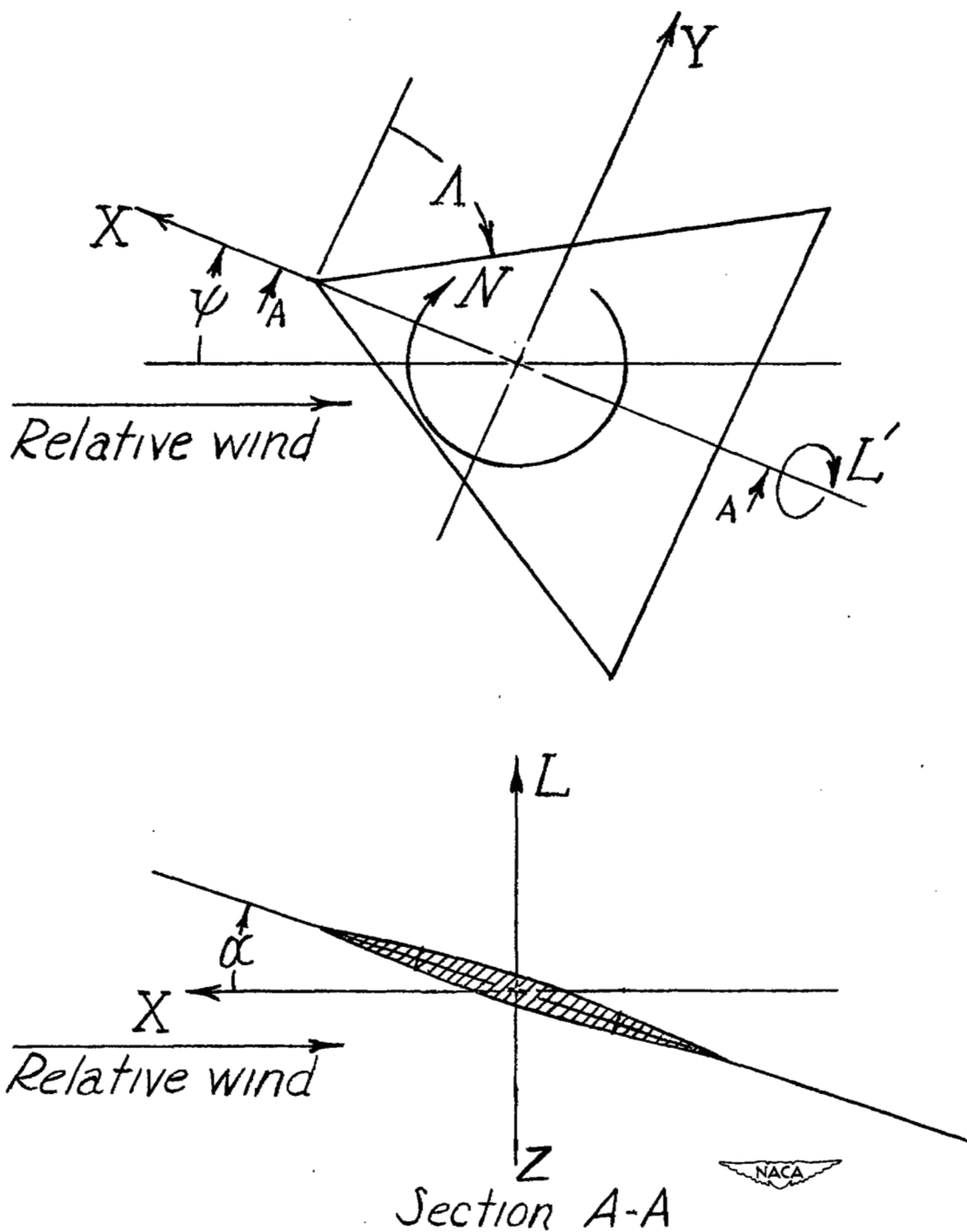
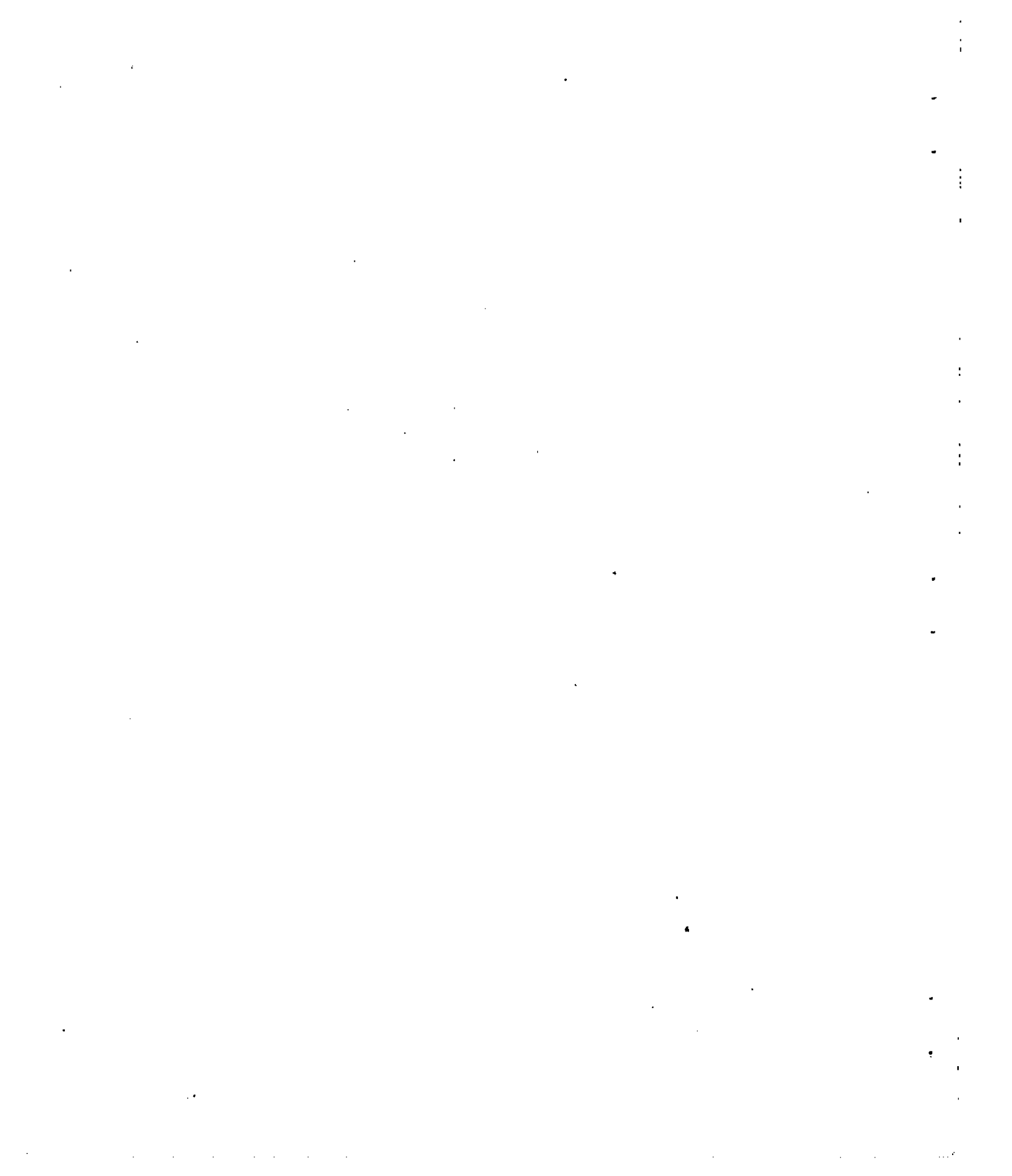
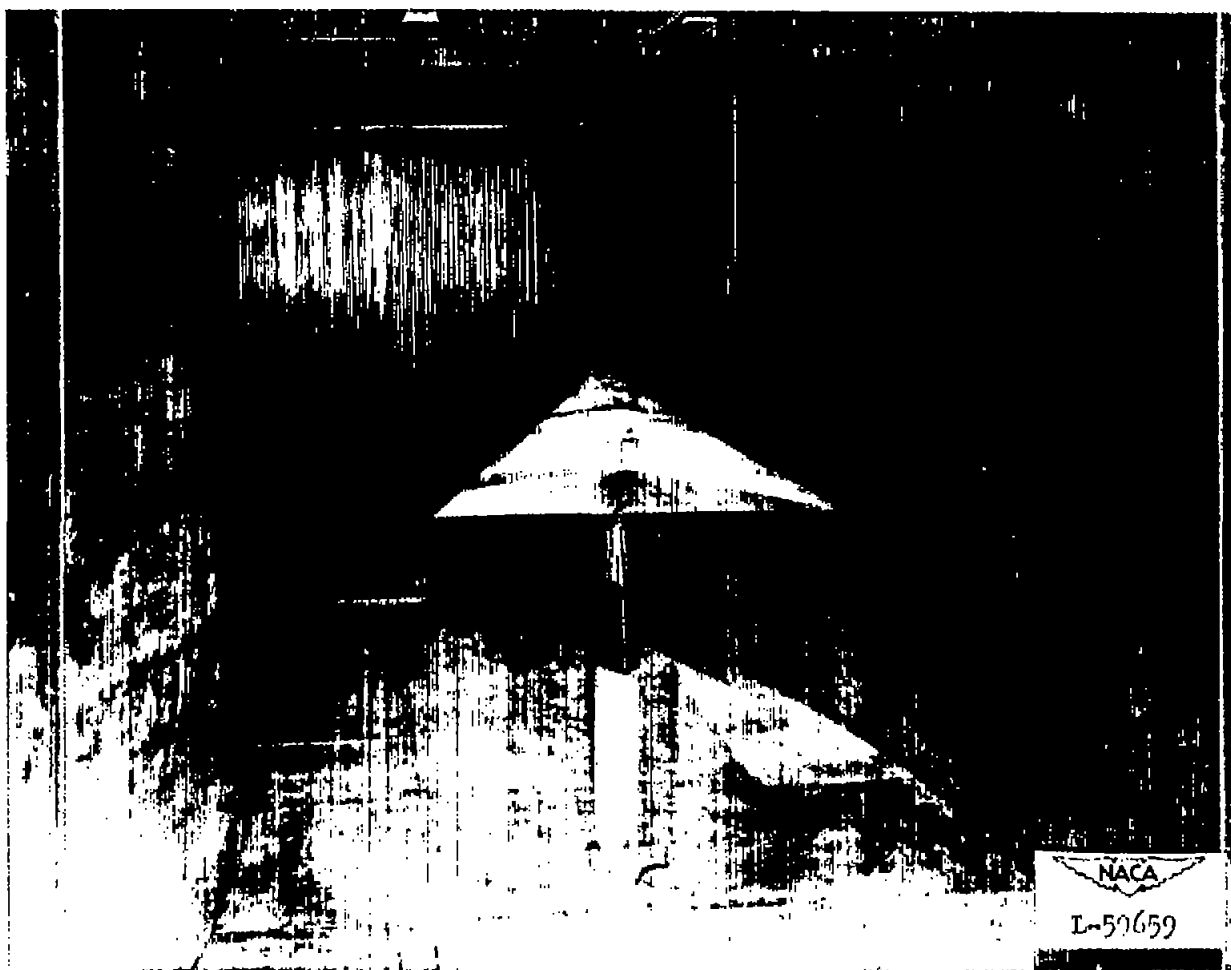


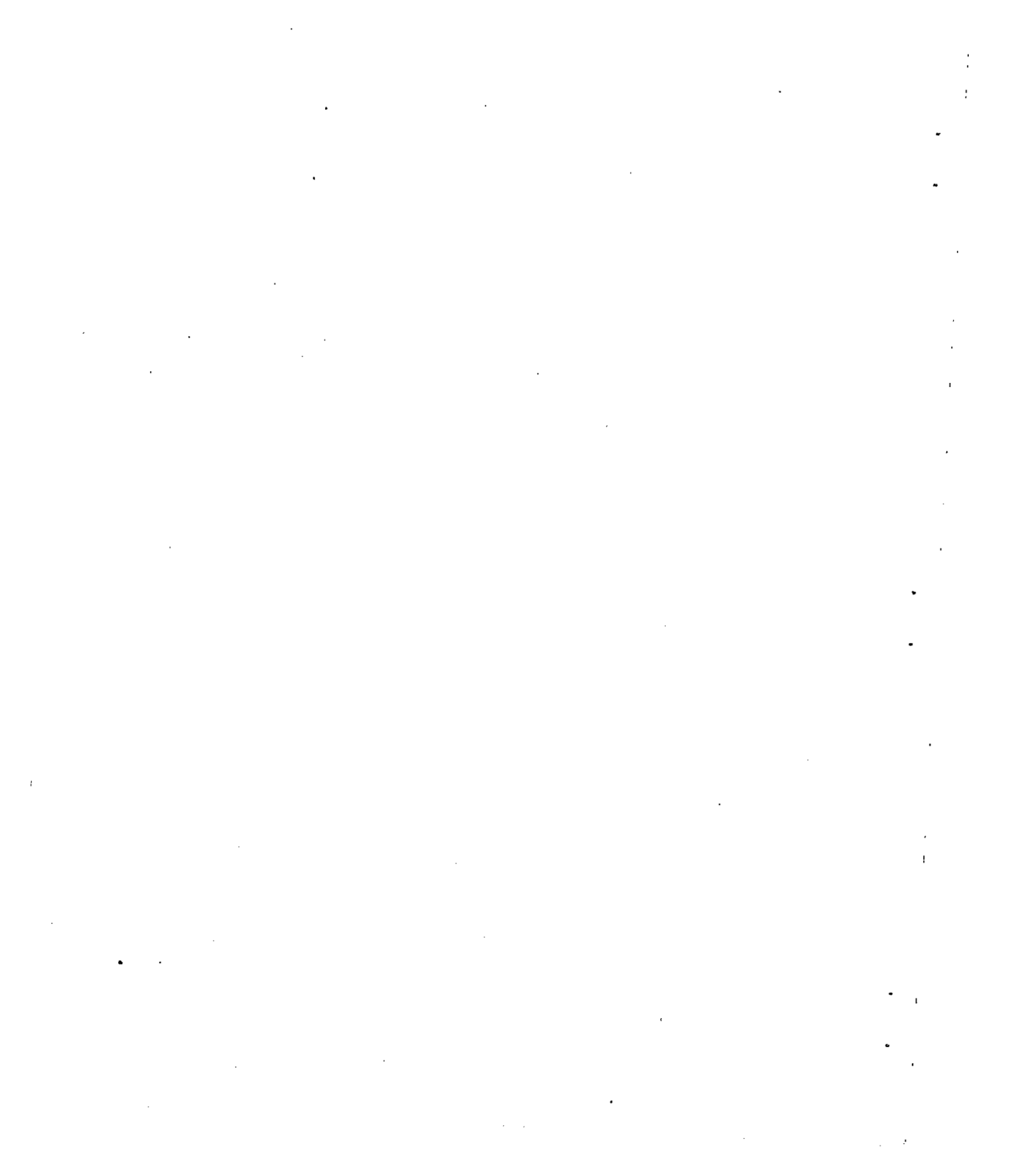
Figure 1.- System of stability axes. Positive forces, moments, and angles are indicated.

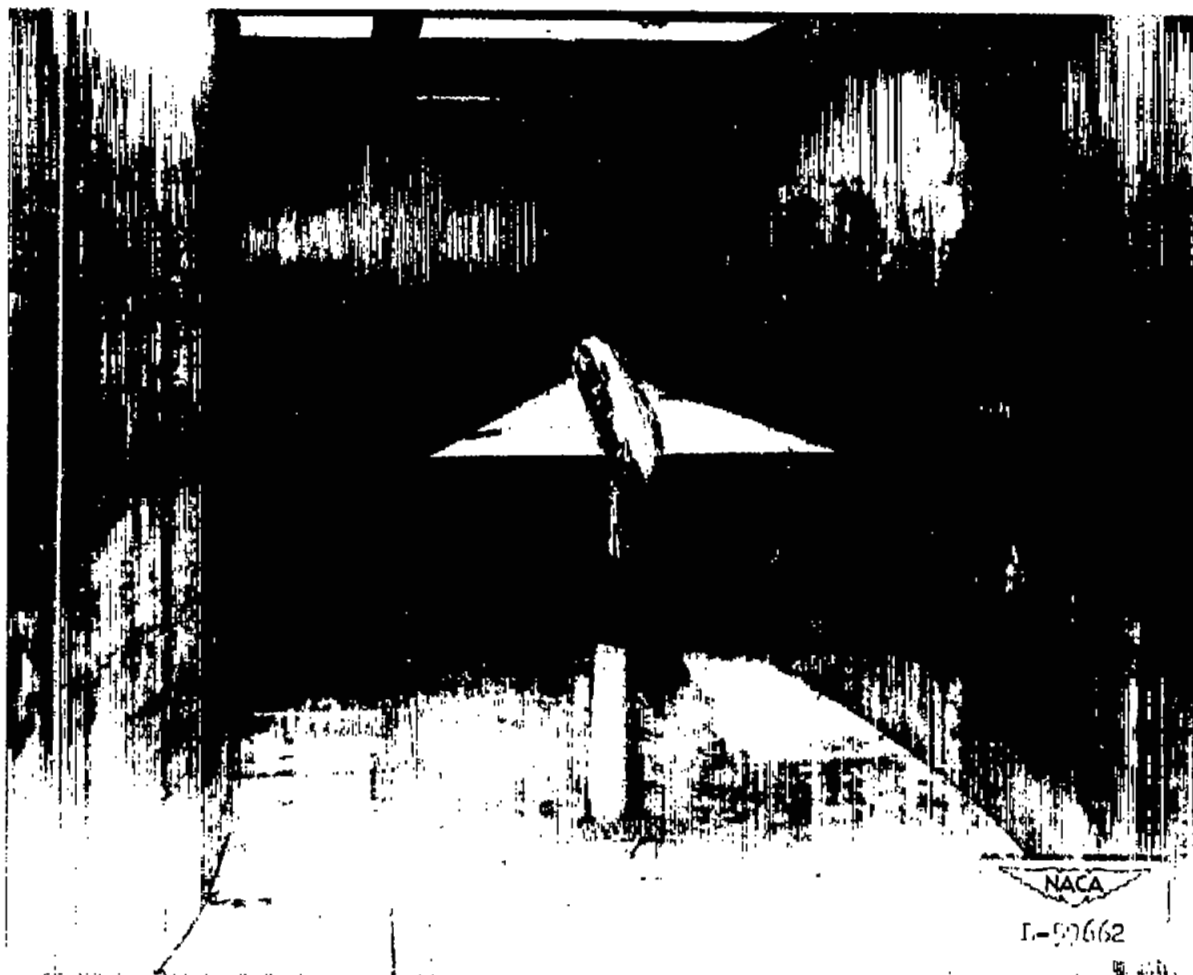




(a) Wing alone. $A = 2.31$; $\Lambda_c/4 = 52.2^\circ$.

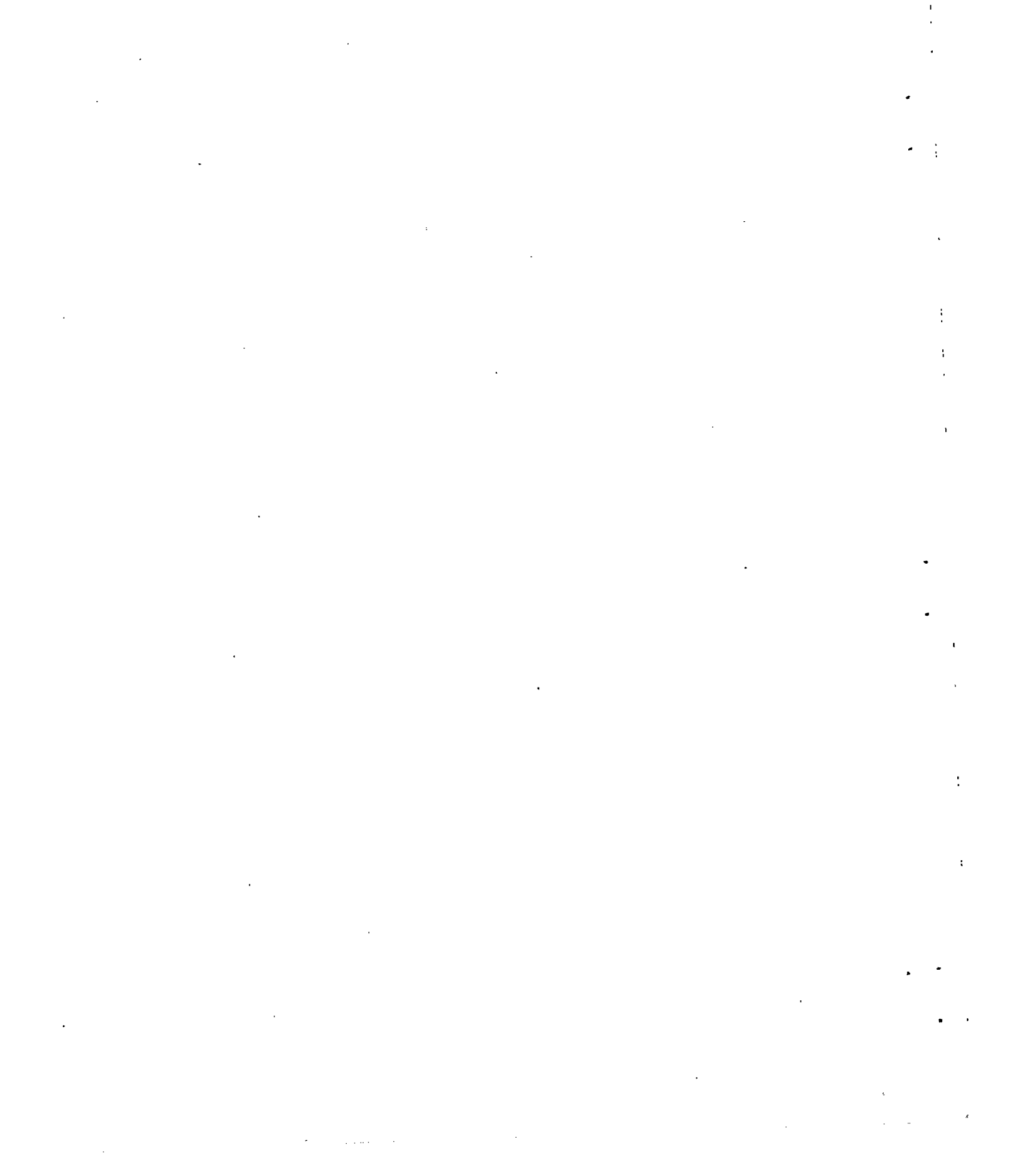
Figure 3.- Triangular-wing model mounted in curved-flow test section of Langley stability tunnel.





(b) Wing and fuselage.

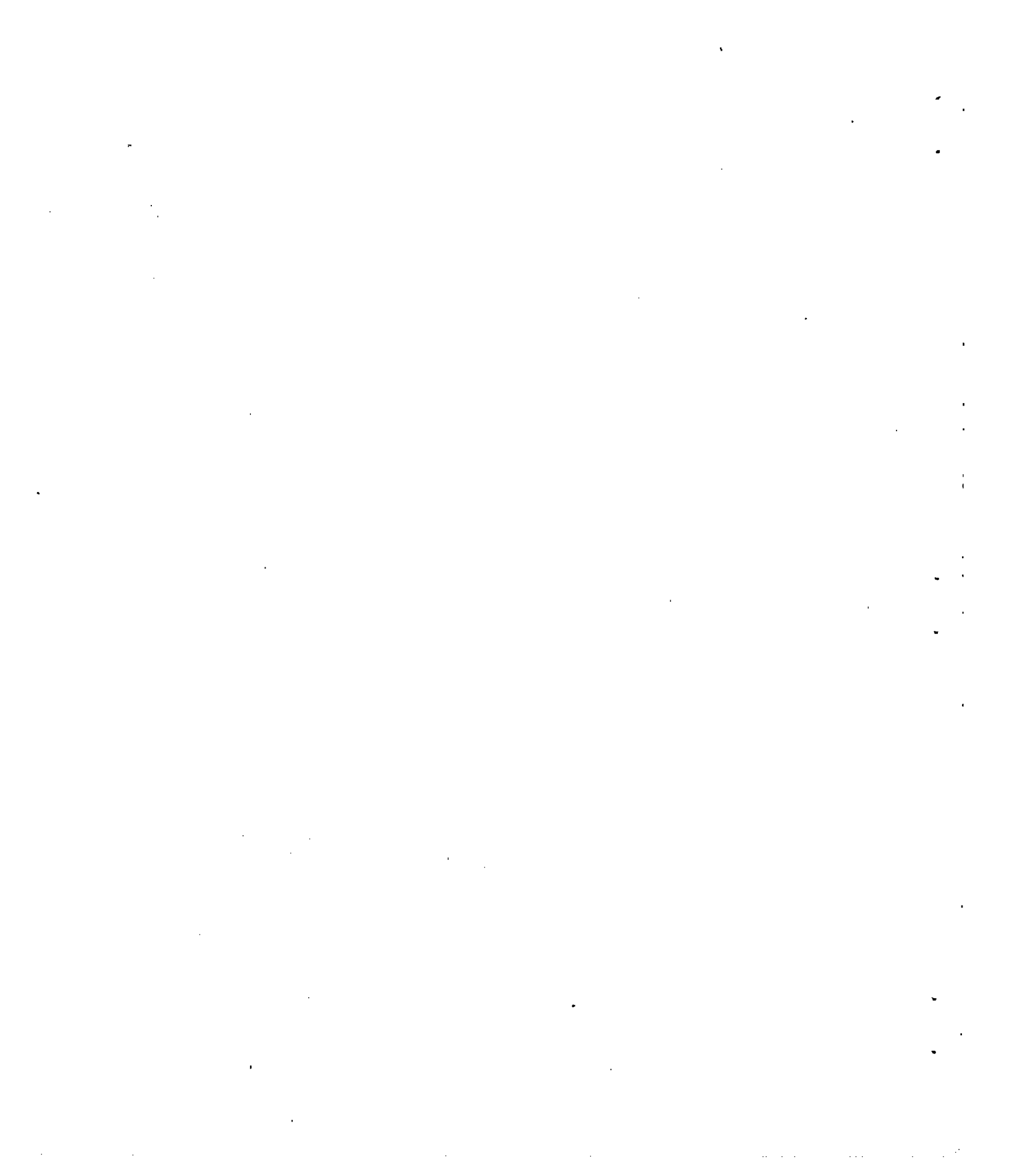
Figure 3.- Continued.

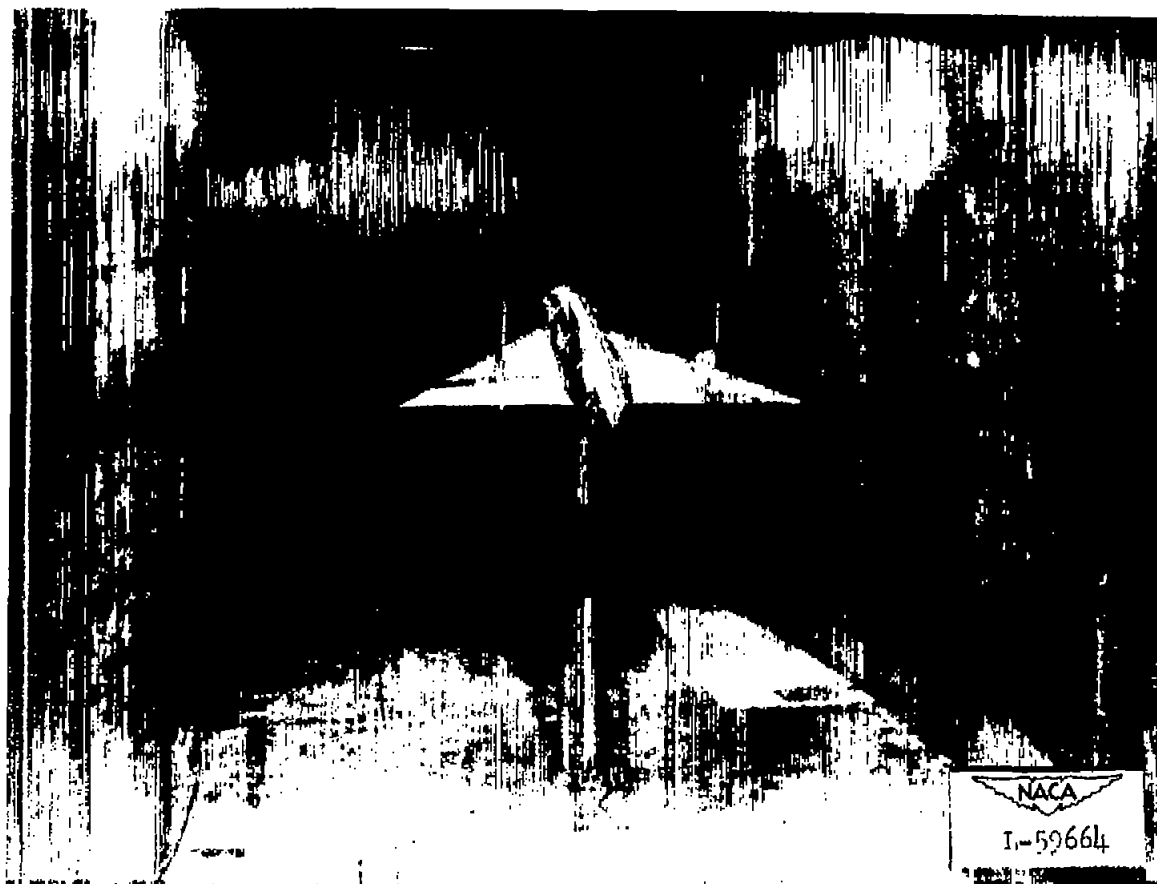




(c) Triangular-wing model with central vertical fin of $A = 2.31$ in rear position. $\frac{S_t}{S_w} = 0.50$.

Figure 3.- Continued.

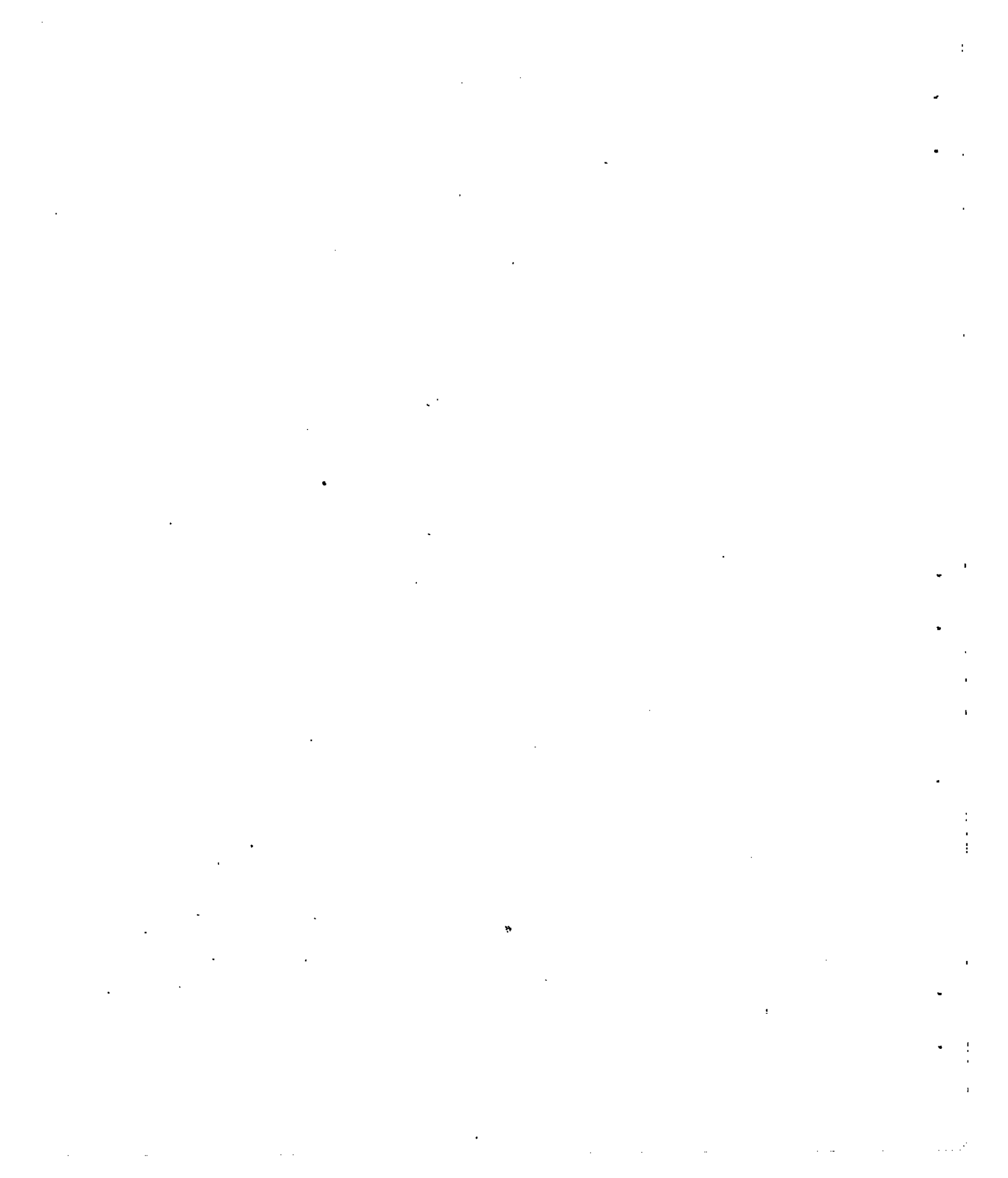


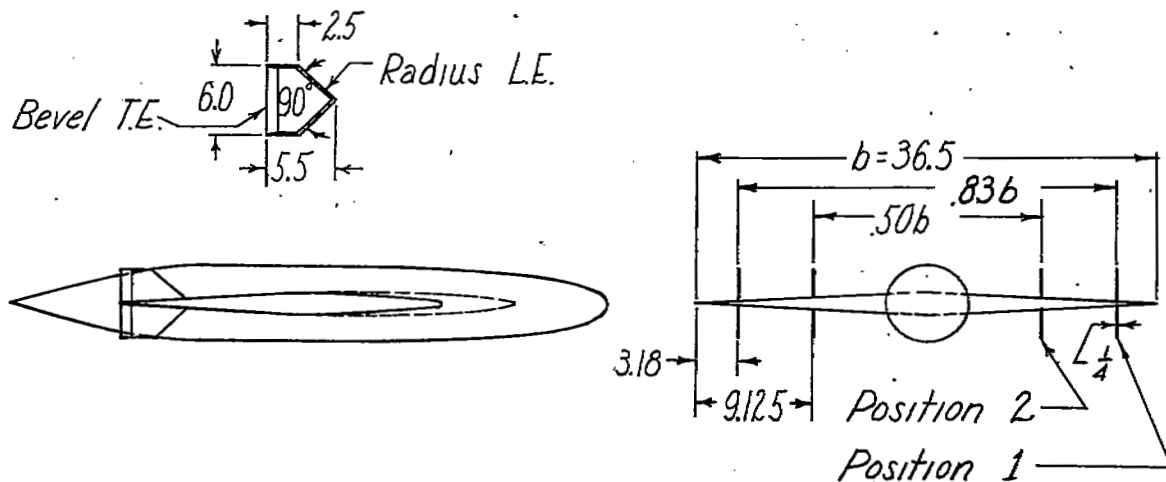


(d) Triangular-wing model with outboard fins of $A = 1.4$ in position 3.

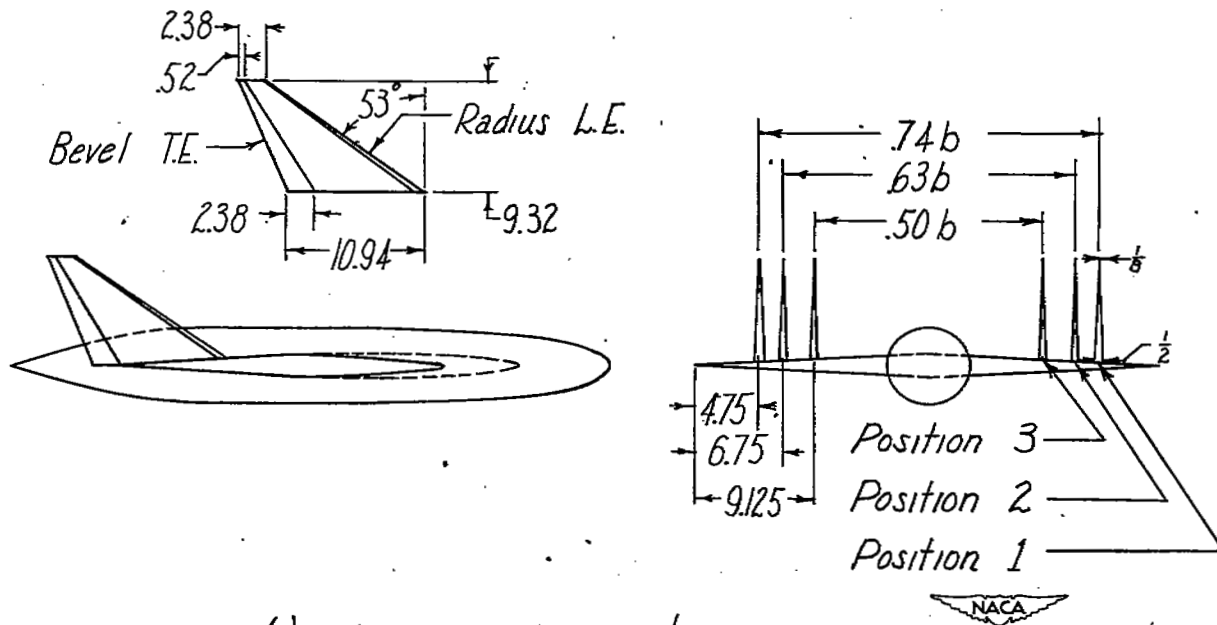
$$\frac{S_t}{S_w} = 0.22.$$

Figure 3.- Concluded.



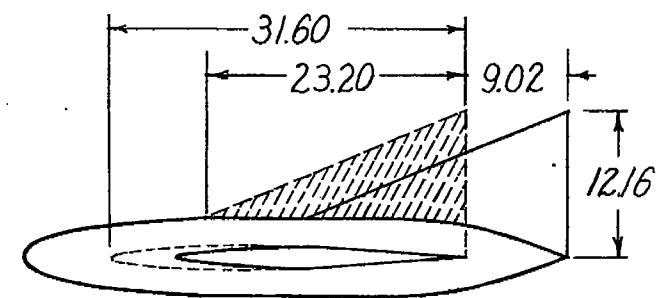


(a) $A=1.5$; $\lambda=0.45$; $S_t/S_W = 0.083$.

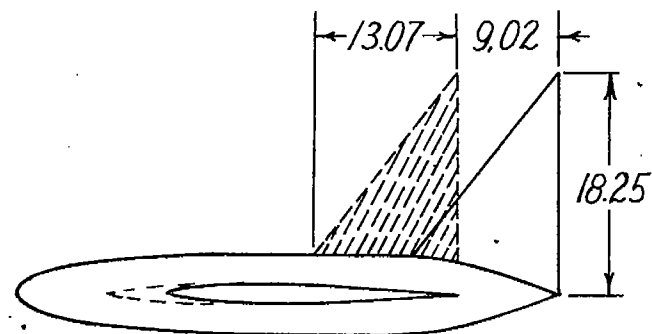


(b) $A=1.4$; $\lambda=0.22$; $S_t/S_W = 0.22$.

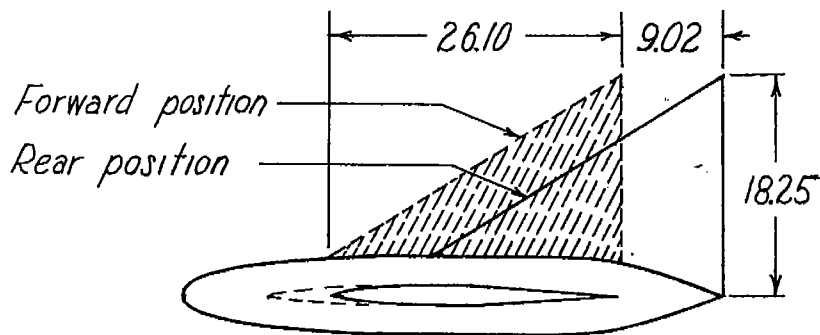
Figure 4.- Positions and dimensions of the outboard fins. All dimensions are in inches unless otherwise specified. Profile of fins, flat plate.



(a) $A=0.77$; $S_t/S_w=0.33$; $\Lambda_{LE}=68.9^\circ$



(c) $A=2.31$; $S_t/S_w=0.25$; $\Lambda_{LE}=40.9^\circ$



(b) $A=1.15$; $S_t/S_w=0.50$; $\Lambda_{LE}=60^\circ$



Figure 5.- Positions and dimensions of the centrally located vertical fins.
All dimensions are in inches.

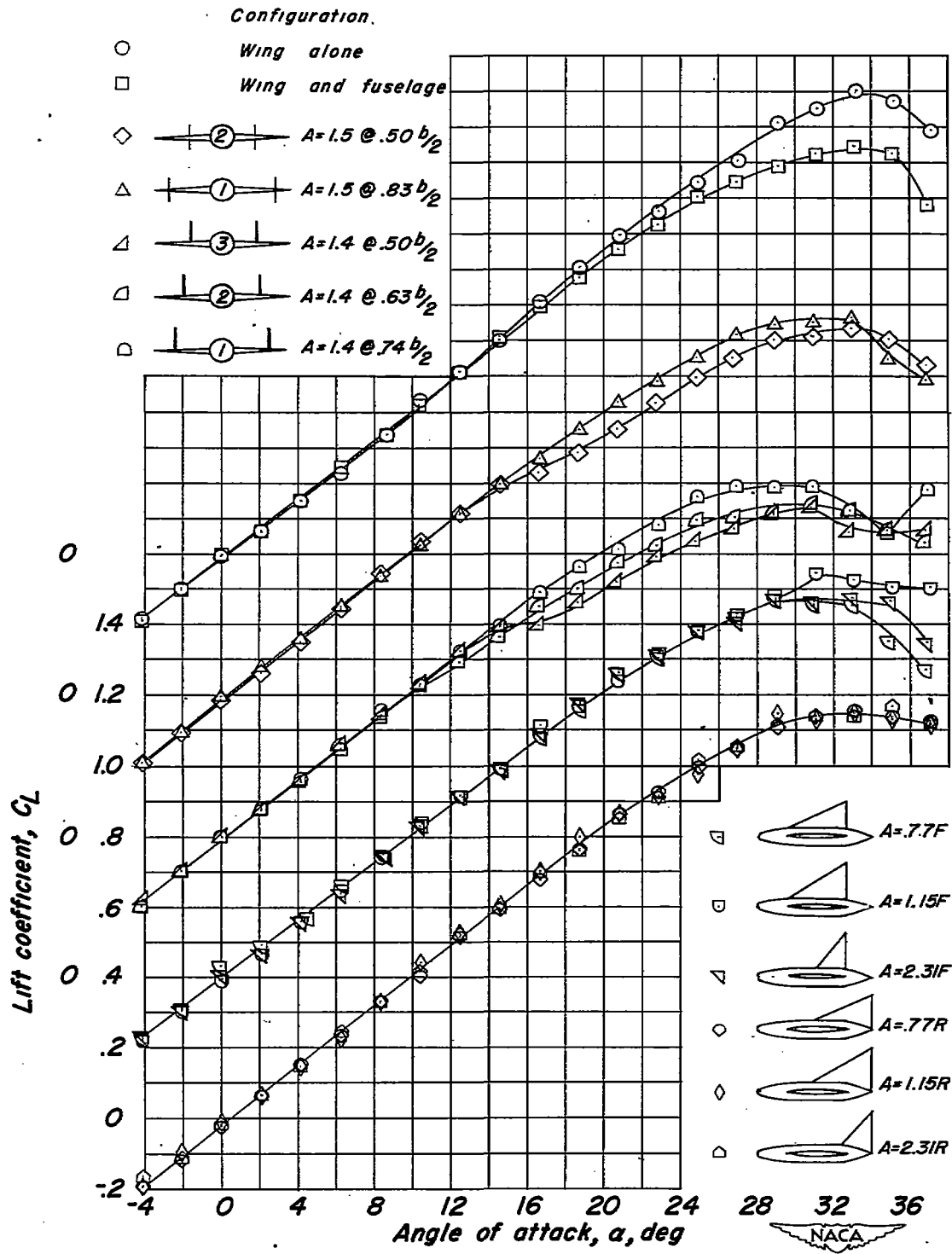


Figure 6.- Variation of C_L with α for a triangular-wing model with various fin configurations.

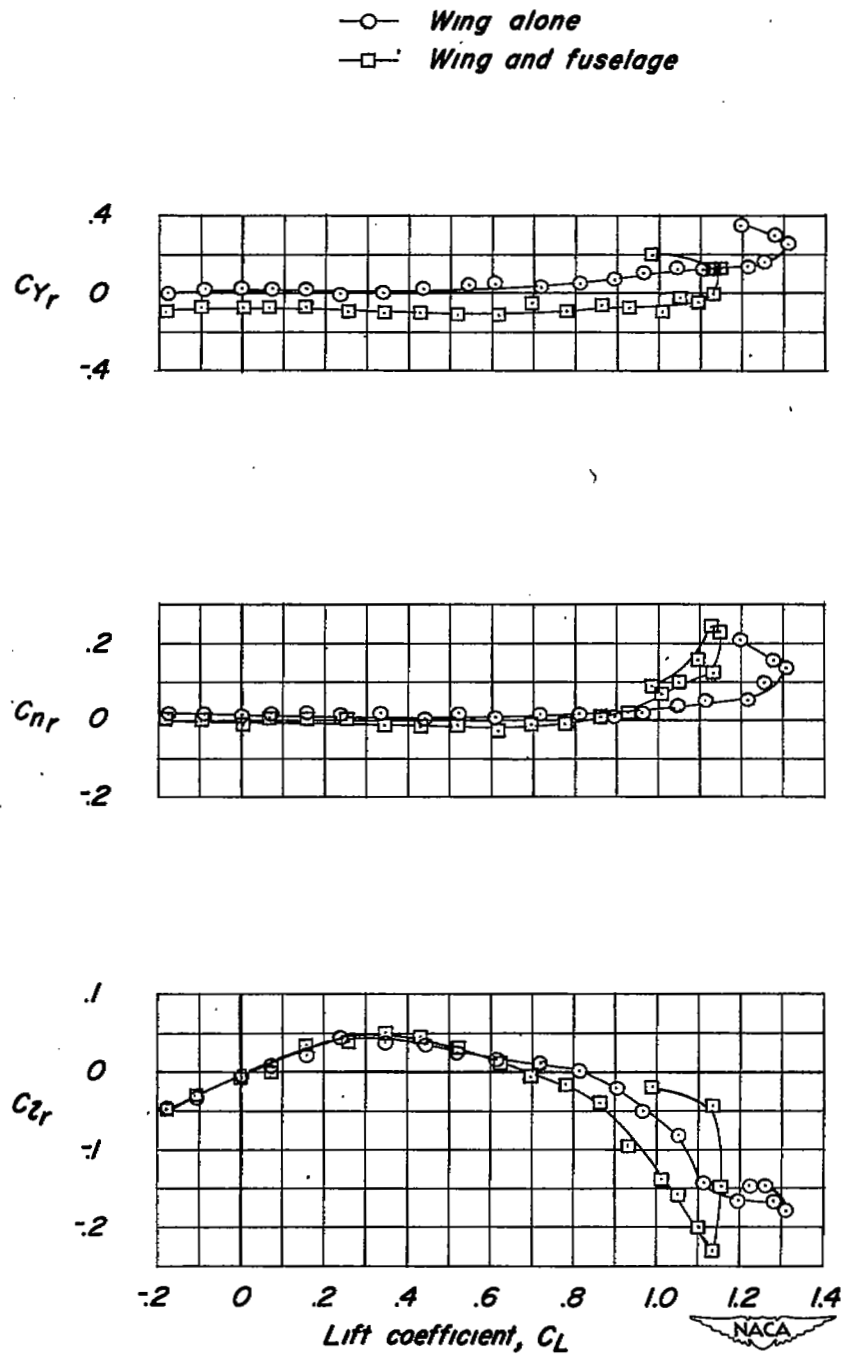


Figure 7.- Variation of C_{Yr} , C_{Nr} , and C_{Lr} with C_L for a triangular wing of aspect ratio 2.31 with and without a fuselage of fineness ratio 7.38; $\Lambda_{c/4} = 52.2^\circ$.

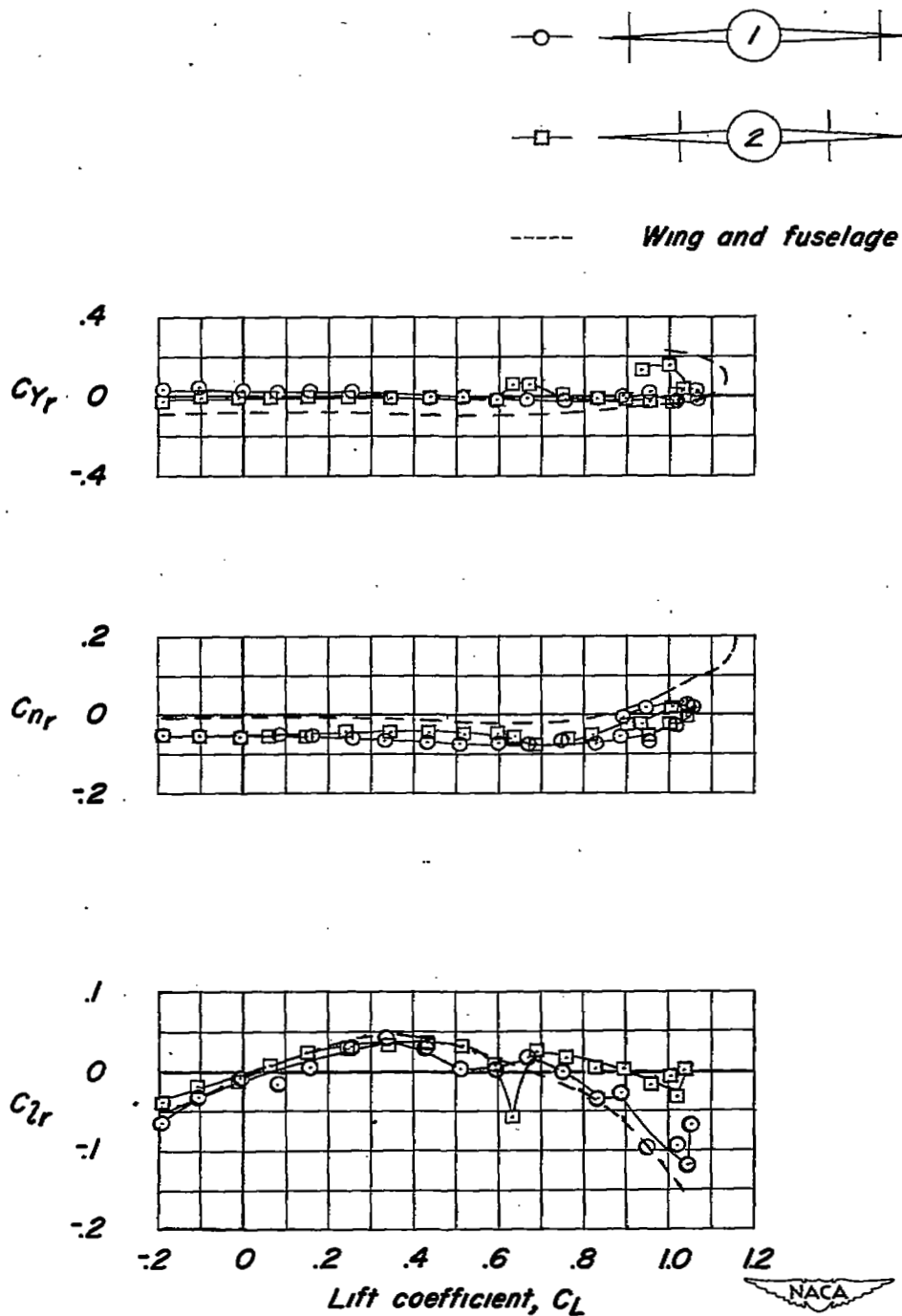


Figure 8.- Effect of outboard fin position on C_{Yr} , C_{Nr} , and C_{Lr} of a triangular-wing model. Fin aspect ratio, 1.5; $\Lambda_{LE} = 45^\circ$; $\lambda = 0.45$; $\frac{S_t}{S_w} = 0.083$.

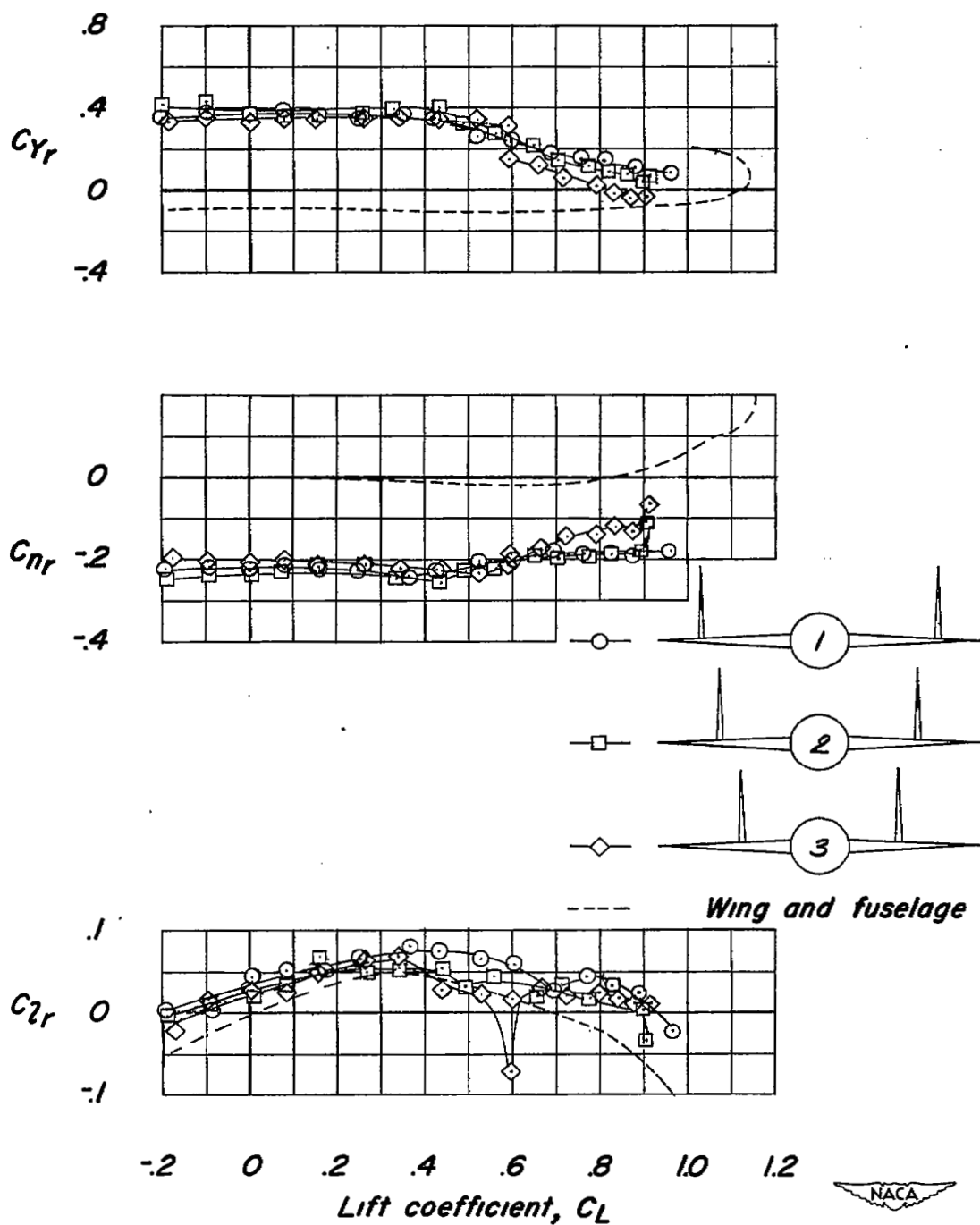


Figure 9.- Effect of outboard fin position on C_{Y_r} , C_{n_r} , and C_{l_r} of a triangular-wing model. Fin aspect ratio, 1.4; $\Lambda_{LE} = 53^\circ$; $\lambda = 0.22$; $\frac{S_t}{S_w} = 0.22$.

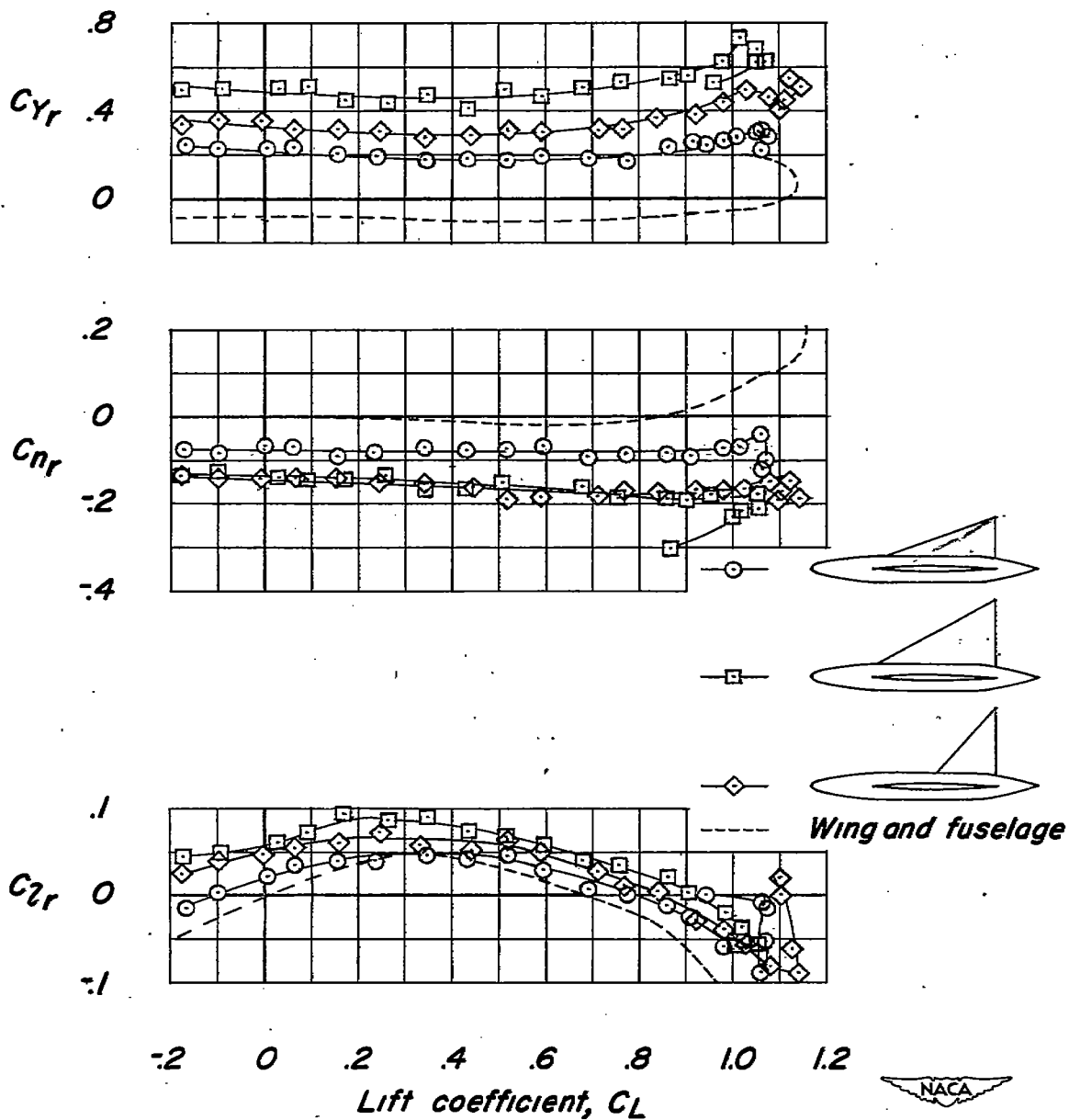


Figure 10.- Effect of central vertical fins on C_{Y_r} , C_{n_r} , and $C_{z_l_r}$ of a triangular-wing model.



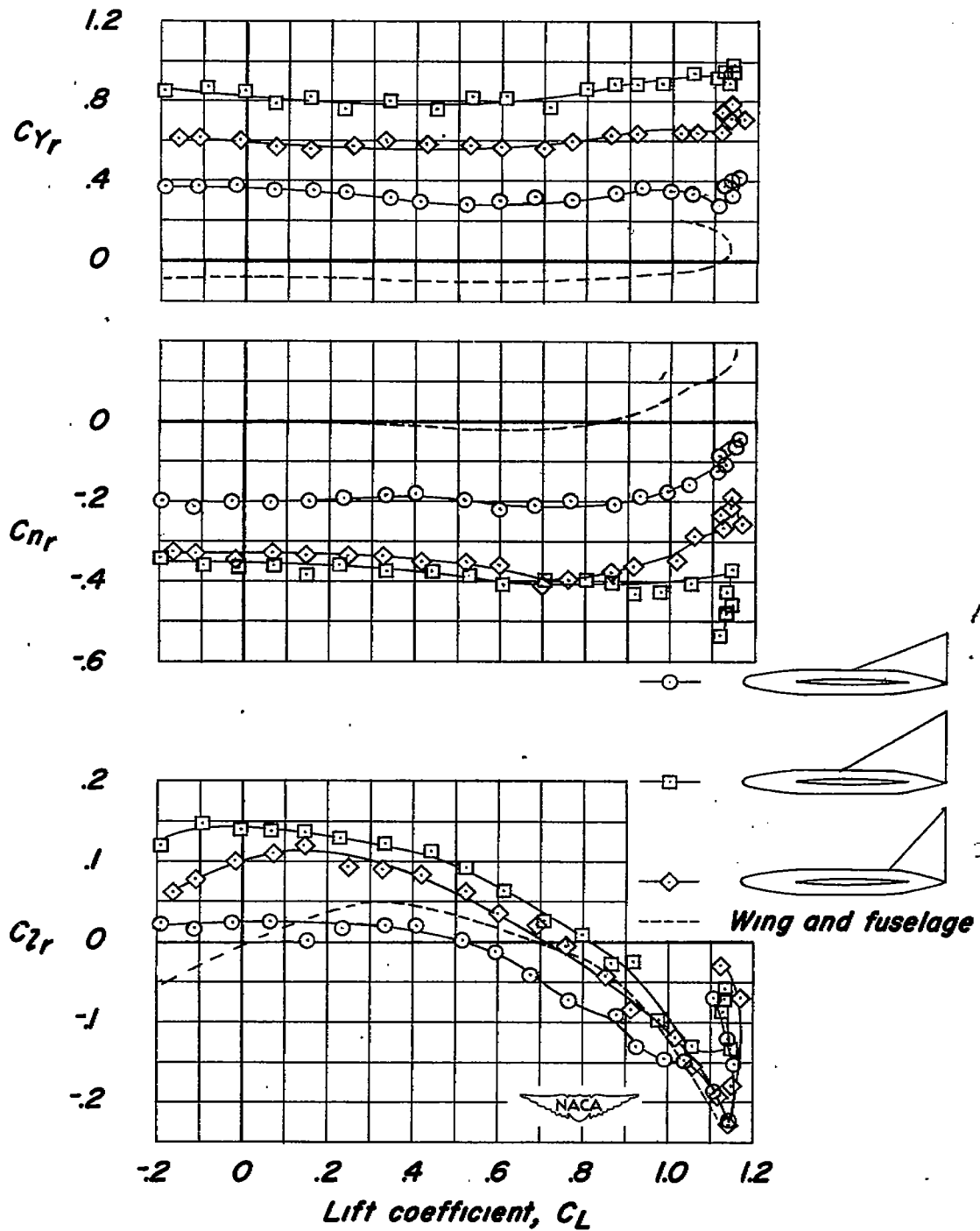
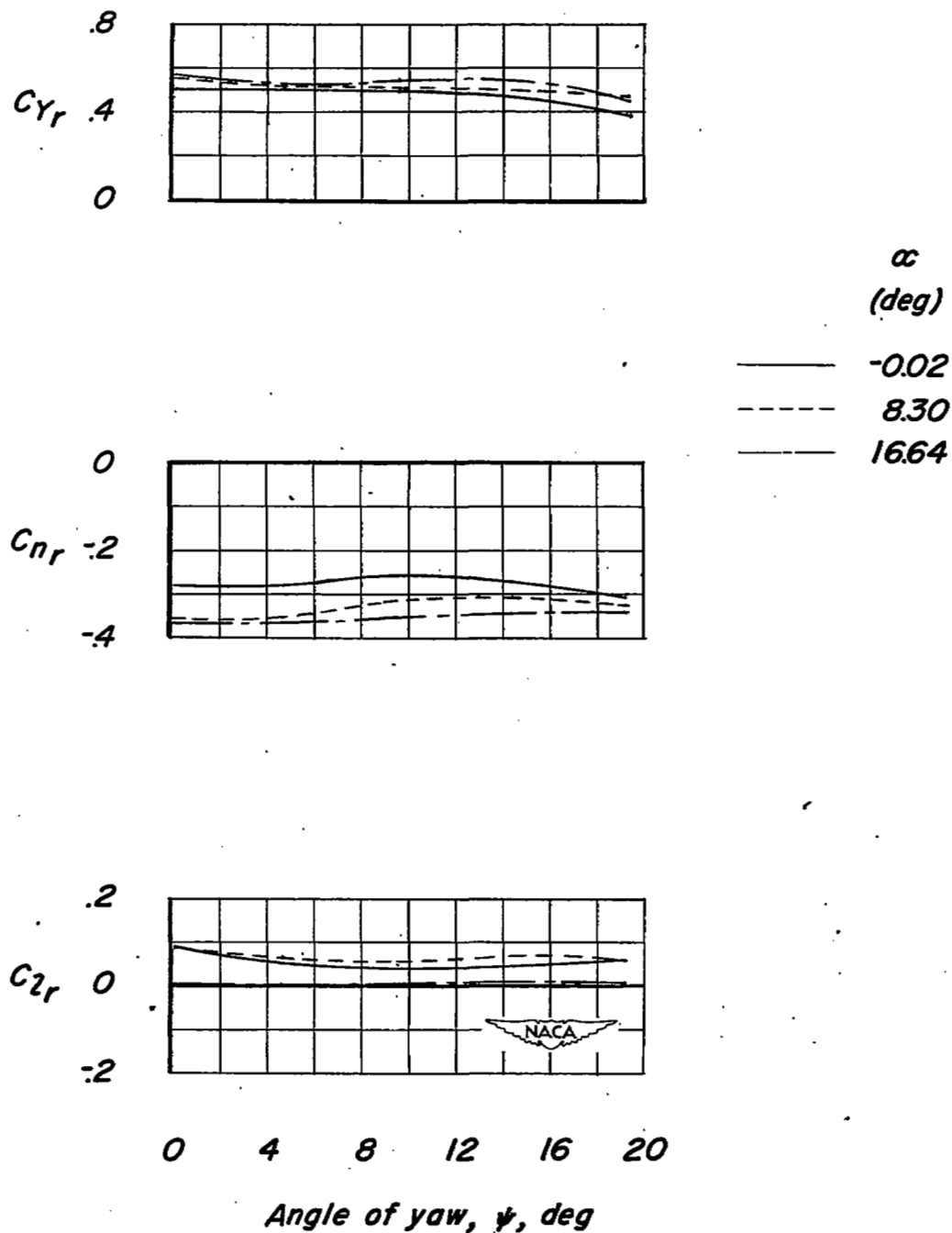
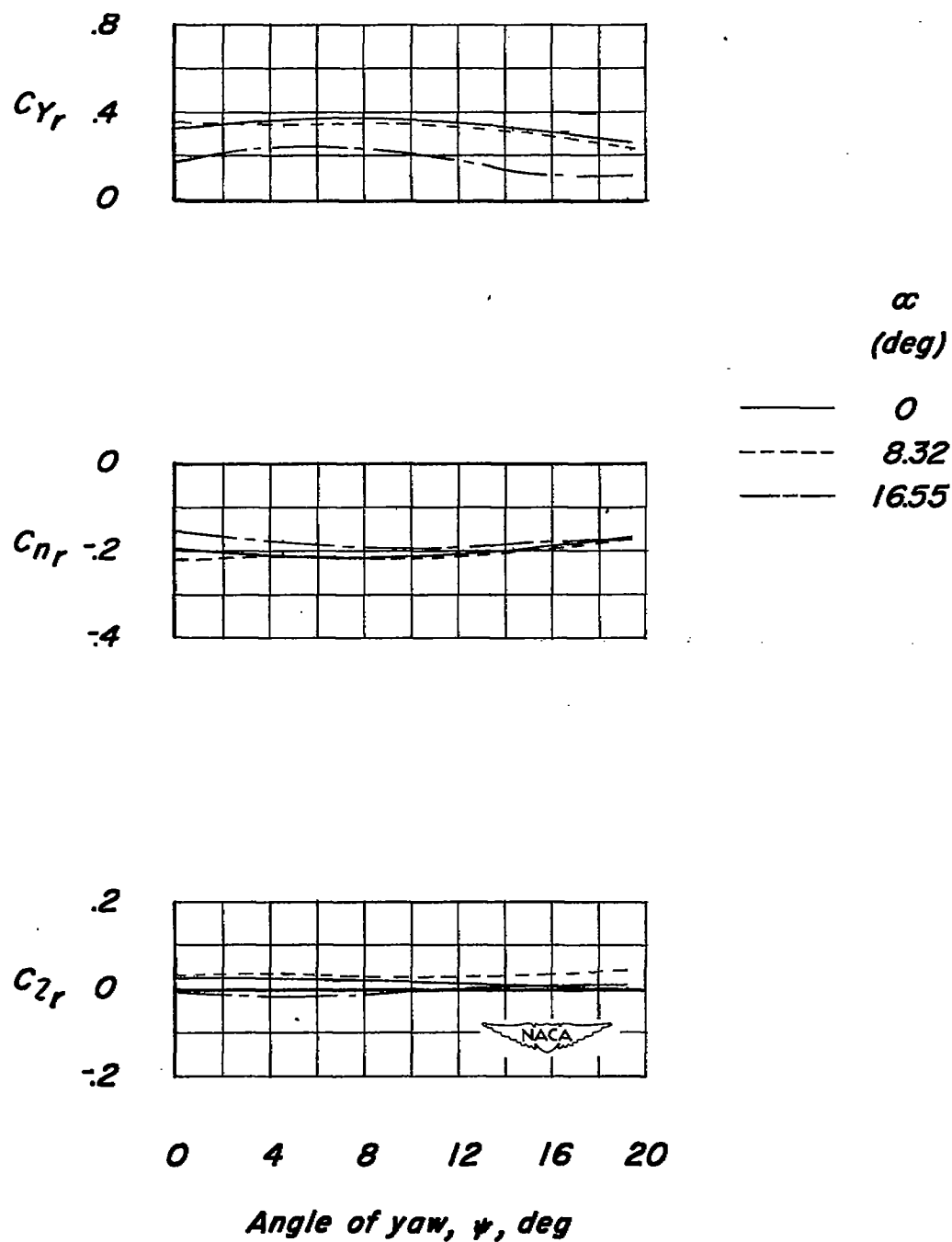


Figure 11.- Effect of central vertical fins on C_{Yr} , C_{nr} , and C_{lr} of a triangular-wing model.



(a) Central fin of $A = 2.31$ in rearward position. $\frac{S_t}{S_w} = 0.25$.

Figure 12.- Variation of C_{Y_r} , C_{N_r} , and C_{L_r} with ψ at several angles of attack for a triangular-wing model.



(b) Outboard fin of $A = 1.4$ in position 3. $\frac{S_t}{S_w} = 0.22$.

Figure 12.- Concluded.

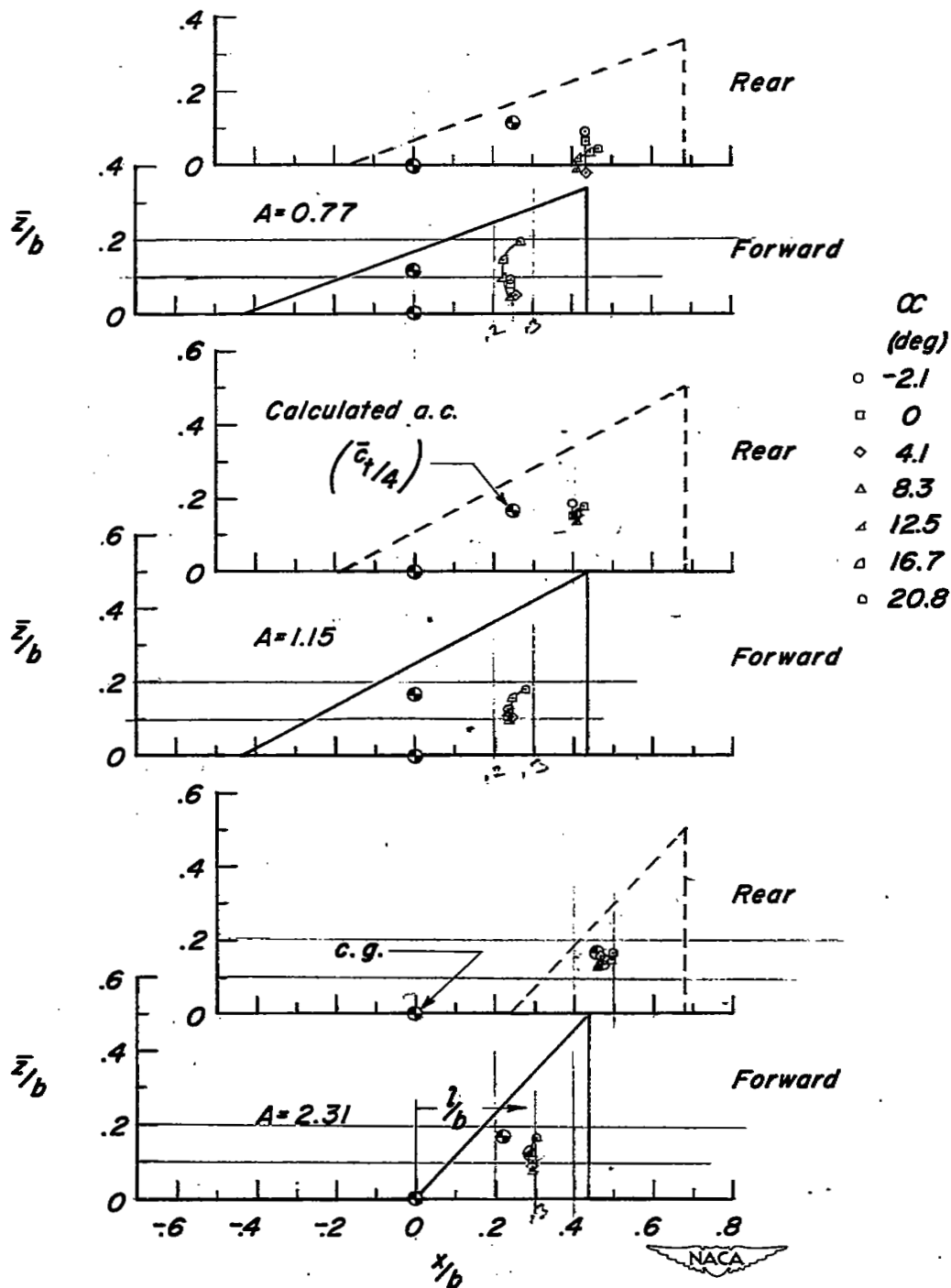


Figure 13.- Effective center of pressure, at several angles of attack, for several central fins on a triangular-wing model.